Geophysical Research Letters

RESEARCH LETTER
10.1029/2023GL106072

Linking Future Tropical Precipitation Changes to Zonally-Asymmetric Large-Scale Meridional Circulation

Dana Raiter[1,2], Eli Galanti[1], Rei Chemke[1], and Yohai Kaspi[1]

[1]Department of Earth and Planetary Sciences, Weizmann Institute of Science, Rehovot, Israel, [2]Presently at Department of Earth and Environmental Sciences, Lamont Doherty Earth Observatory, Columbia University, New York, NY, USA

Abstract Projected tropical precipitation changes by the end of the century include increased net precipitation over the Pacific Ocean and drying over the Indian Ocean, prompting ongoing debate about the underlying mechanisms. Previous studies argued for the importance of the zonal circulation in the longitudinally dependent tropical precipitation response, as the meridional circulation is often defined and analyzed as the zonal mean. Here we show that the projected changes in the meridional circulation are highly longitudinally dependent, and explain the zonally dependent changes in net precipitation. Our analysis exposes a zonal shift in the ascending branch of the meridional circulation, associated with a strengthened net precipitation over the central Pacific and weakened precipitation in the Indo Pacific. The zonal circulation has minor influence on these projected tropical precipitation changes. These results point to the importance of monitoring the longitudinal changes in the meridional circulation for improving our preparedness for climate change impacts.

Plain Language Summary Under global warming precipitation patterns are expected to change. Substantial changes will occur in the tropics, where an increase in precipitation over the Pacific Ocean and drying over the Indian Ocean are expected. In spite of the immense climate impacts of this phenomenon, the mechanisms underlying these changes have remained unknown. This study elucidates on the mechanism controlling this change, connecting the expected precipitation changes to the large-scale tropical circulation. By separating the three-dimensional tropical circulation into its components along the north-south and east-west directions, we show that the spatial changes in north-south circulation explain most of the projected change in tropical precipitation, while the east-west circulation has little to no effect. These results are further supported by analysis of the future changes of tropical air mass trajectories.

Key Points:

- Climate change models project a significant precipitation increase over the tropical Pacific and drying over the tropical Indian Ocean
- The projected changes in the large-scale longitudinally dependent meridional circulation can explain these precipitation/drying changes
- We support these results with a coupled Eulerian-Lagrangian analysis, stressing the importance of treating the large-scale circulation as 3D

Supporting Information:

Supporting Information may be found in the online version of this article.

Correspondence to:

D. Raiter,
dana.raiter@columbia.edu

Citation:

Raiter, D., Galanti, E., Chemke, R., & Kaspi, Y. (2024). Linking future tropical precipitation changes to zonally-asymmetric large-scale meridional circulation. *Geophysical Research Letters*, *51*, e2023GL106072. https://doi.org/10.1029/2023GL106072

Received 24 AUG 2023
Accepted 14 FEB 2024

1. Introduction

The overall global precipitation is expected to increase by the end of the 21st century, however, it is anticipated to vary drastically across different regions and climate zones (Collins et al., 2013). For example, in the deep tropics, climate model projections suggest the zonally averaged net precipitation (precipitation minus evaporation) will increase, while in the subtropics, a decrease is expected. The precipitation changes are also projected to exhibit significant longitudinal variability. For example, the response of net precipitation to global warming is predicted to be stronger over the ocean than over land (Byrne & O'Gorman, 2015). Previous studies suggested several mechanisms for these changes, including both thermodynamic and dynamic processes (Byrne & O'Gorman, 2015; Chadwick et al., 2013; Held & Soden, 2006; Seager et al., 2010). Thermodynamically induced precipitation changes assume negligible changes in the circulation (e.g., the wet-gets-wetter dry-gets-drier mechanism) (Byrne & O'Gorman, 2015; Chou & Neelin, 2004; Held & Soden, 2006), while dynamically induced precipitation changes are driven by variations in the large-scale atmospheric circulation (Chou et al., 2009; Karnauskas & Ummenhofer, 2014; Vecchi & Soden, 2007).

One of the most significant changes in precipitation occurs in the deep tropics, where climate models predict a robust strengthening of net precipitation in the equatorial Pacific, and drying in the Indo-Pacific (Figure 1). This zonal asymmetry has been previously attributed to changes in the Walker circulation (Seager et al., 2010; Vecchi & Soden, 2007). However, these studies used the traditional definition of the zonally averaged meridional circulation, which is inherently zonally symmetric and fails to reveal its zonal asymmetries (Figure S1 in Supporting Information S1).

Recent studies analyzing the large-scale regional meridional circulation find it to vary substantially with longitude (Karnauskas & Ummenhofer, 2014; Nguyen et al., 2018; Schwendike et al., 2014; Zhang & Wang, 2013). In

10.1029/2023GL106072

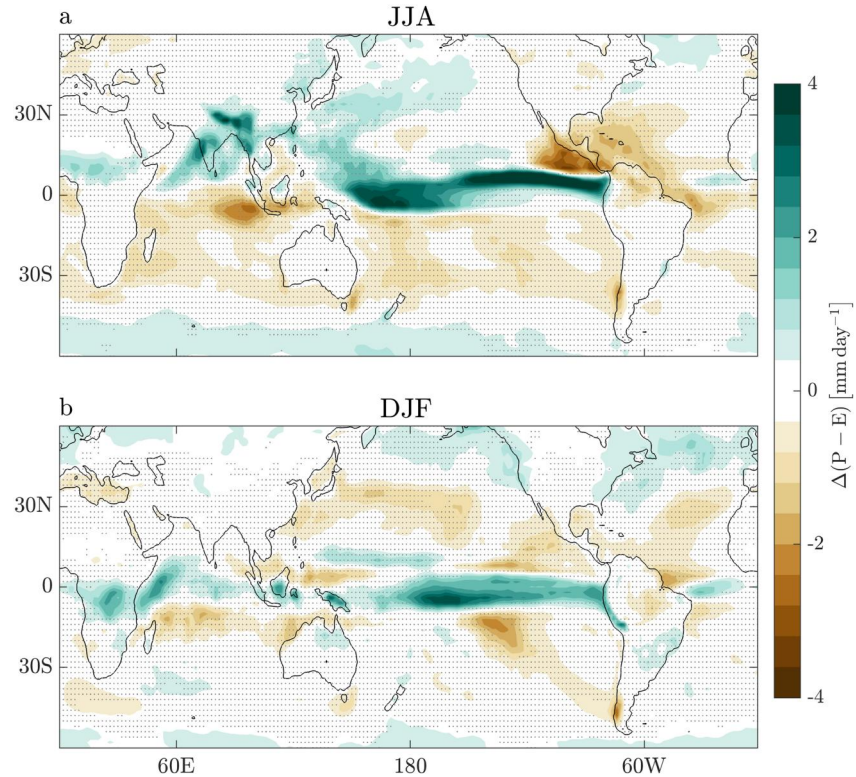

Figure 1. Projected changes (difference between the 2080–2099 and 1980–1999 periods) in precipitation minus evaporation (P–E) for (a) June-July-August (JJA) and (b) December-January-February (DJF) in the mean of CMIP6 models, under SSP5-8.5 and historical scenarios. Contour interval is 0.4 mm day^{-1}. The small black dots indicate regions where the net precipitation changes are statistically not significant at the 5% level based on a Student's *t*-test.

particular, the tropical large-scale circulation is revealed to be inherently three-dimensional, and can be described as an atmospheric conveyor belt. In the lower levels, the air converges into the Indo-Pacific warm pool, ascends, and moves westward and poleward, while at higher altitudes, before merging into the jet stream and moving eastward, it finally descends in the east and converges back into the warm pool (Raiter et al., 2020). This zonally asymmetric circulation was also found to vary considerably on interannual time scales (e.g., Galanti et al., 2022; Schwendike et al., 2014). Furthermore, in response to increasing greenhouse gases, the expansion of the Hadley circulation (Chemke & Polvani, 2019; Collins et al., 2013; Lu et al., 2007; Vallis et al., 2015; Waugh et al., 2018) was shown to significantly vary across longitudes (Lucas & Nguyen, 2015; Staten et al., 2019). Other studies showed zonal variations in the Intertropical Convergence Zone response to global warming (Mamalakis et al., 2021). Thus, to improve our understanding of the climate impacts of anthropogenic emissions in the deep tropics, it is imperative to not only account for the zonal circulation changes, but also to examine the longitudinally dependent meridional circulation.

2. Methods

2.1. CMIP6 Models

In this study we use 31 models from Phase 6 of the Coupled Model Intercomparison Project (CMIP6) (Eyring et al., 2016). The list of models can be found in Table S1 in Supporting Information S1. All models are forced with the historical forcing for the years 1980–1999 and the Shared Socioeconomic Pathway 5–8.5 (SSP5-8.5) forcing for the years 2080–2099; we use the "r1i1p1f1" member, in order to weigh all models equally. Models are interpolated to a 2° × 2° grid.

2.2. Defining the Meridional Circulation

The Hadley Circulation is traditionally defined as the zonally averaged meridional circulation calculated via $\psi(\theta,p,t) = \frac{2\pi a \cos\theta}{g}\int_0^p [v](\theta,p,t)dp$ (Hartmann, 2016), where v is the meridional velocity and brackets denote zonal average. θ, p, t are the latitude, pressure and time, respectively, a is the radius of the Earth and g is the gravitational acceleration. Figure S1 in Supporting Information S1 illustrates the 20th and 21st centuries zonally averaged meridional circulation, for the annual mean, June to August (JJA) and December to February (DJF).

To decompose the vertical velocity (ω) to its meridional-related component (ω_θ, i.e., the vertical motion of air in the meridional circulation), and the zonal-related component (ω_ϕ, i.e., the vertical motion of air in the zonal circulation) (Figures 2c and 2d), we follow previous studies (Keyser et al., 1989; Schwendike et al., 2014), and define the vertical velocity using a potential function μ,

$$\nabla^2\mu = -\omega. \tag{1}$$

We then calculate the meridional (ω_θ) and the zonal (ω_ϕ) components of the vertical velocity as follows,

$$\omega_\theta \cos\theta = \frac{1}{a^2}\frac{\partial}{\partial\theta}\left(\cos\theta\frac{\partial\mu}{\partial\theta}\right),\ \omega_\phi \cos\theta = \frac{1}{a^2\cos\theta}\frac{\partial^2\mu}{\partial\phi^2}, \tag{2}$$

where ϕ is longitude.

Similar to the vertical velocity decomposition, we use the Helmholtz decomposition and decompose the horizontal velocity field into rotational and divergent components for analyzing the longitudinally dependent meridional circulation (also known as the local Hadley circulation) (Hu et al., 2017; Keyser et al., 1989; Schwendike et al., 2014). This enables the investigation of the future longitudinal-dependent expansion of the tropical circulation. Initially, we calculate the divergence of the horizontal wind ($\mathbf{v} = (u,v)$) on constant pressure surfaces

$$D = \nabla\cdot\mathbf{v}. \tag{3}$$

Subsequently, by taking the gradient of the velocity potential, $\nabla^2\chi = D$, we calculate the divergent horizontal wind ($\mathbf{v}_{\text{div}} = (u_{\text{div}}, v_{\text{div}})$)

$$\nabla\chi = \mathbf{v}_{\text{div}}. \tag{4}$$

Finally, we calculate the longitudinally dependent meridional circulation (ψ_H) and the latitudinally dependent zonal circulation (ψ_W), using the divergent component of the meridional velocity and the divergent component of the zonal velocity, respectively:

$$\psi_H(\phi,\theta,p,t) = \frac{1}{g}\int_0^p v_{\text{div}}\left(\phi,\theta,p',t\right)dp', \psi_W(\phi,\theta,p,t) = \frac{1}{g}\int_0^p u_{\text{div}}\left(\phi,\theta,p',t\right)dp'. \tag{5}$$

We opt for the divergent component, as it represents the non-rotational component, crucial because it participates in the vertical direction, unlike the rotational wind, which is confined to the horizontal plane (e.g., Raiter et al., 2020). One caveat of this decomposition method is that a meridional circulation may occur even if the horizontal wind is predominantly zonal (Fuselier & Wright, 2009). However, this scenario is less relevant for the deep tropics.

Figure S2 in Supporting Information S1 shows the projected changes in the longitudinally dependent meridional circulation (colored contour) with the historical values for reference (black contours, dashed lines are negative values and solid lines are positive values). Agreement in sign between black and colored contours indicates strengthening of the circulation, while opposite signs signify weakening. Note that alternatively the longitudinally dependent meridional circulation can be calculated via the integral of ω_θ with respect to latitude since the horizontal and vertical velocities are connected through the continuity equation and the velocity potential, χ, can be calculated via: $\chi = \partial\mu/\partial p$. The response of the potential function at 200 hPa is shown in Figure S3 in Supporting Information S1. To evaluate the statistical significance of our results, we utilize an independent two-sample t-test with unequal variances, at a 95% confidence level.

2.3. Lagrangian Analysis–Calculating Trajectories of Air Parcels

The trajectories are calculated by numerically solving the trajectory equation: $\frac{D\mathbf{x}}{Dt} = \mathbf{u}(\mathbf{x})$, where $\mathbf{x}$ is the location of the air parcel ($\mathbf{x} = (x,y,z)$), and $\mathbf{u}$ is the time averaged three-dimensional velocity field ($\mathbf{u} = (u,v,w)$). For each time step Δt, we calculate a new location using the three-dimensional velocity field

$$\mathbf{x}^* = \mathbf{x} + \mathbf{u}(\mathbf{x})\Delta t, \tag{6}$$

with $\Delta t = 6$ hr. The air parcels are then followed for 20 days. Note that we use the time-averaged velocity field rather than the average of trajectories calculated from the instantaneous wind.

3. Results

3.1. Spatial Shifts of the Dynamically Driven Precipitation Changes

We start by examining the response (difference between the 2080–2099 and 1980–1999 periods) of net precipitation (precipitation minus evaporation, P–E), in CMIP6 forced under the historical (20th century) and the SSP5-8.5 scenario (21st century). During JJA, a zonal shift in the net precipitation is projected to occur in the deep

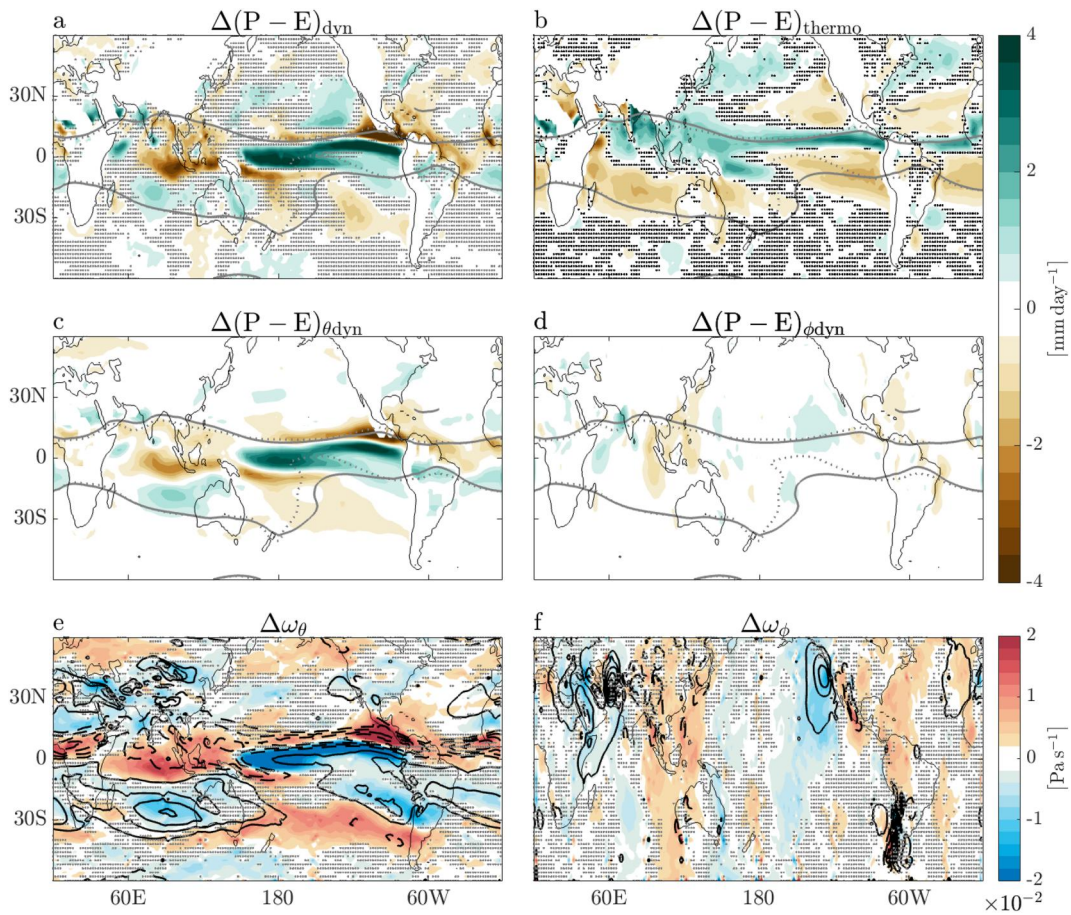

Figure 2. (a) Dynamic and (b) thermodynamic components of the projected changes in P–E (colored contours) for JJA. Gray solid and dotted contours indicate the edge of longitudinally dependent meridional circulation calculated over the 2080–2099 and 1980–1999 periods, respectively. (c) The meridional and (d) zonal contributions of the divergent wind to the dynamic component of the projected changes in P–E. Projected changes in 500 hPa vertical velocity associated with the (e) meridional ($\Delta\omega_\theta$) and (f) zonal ($\Delta\omega_\phi$) circulation. In panels e and f the dashed and solid lines, respectively, represent negative and positive values over the 1980–1999 period. Colored contour interval is 2×10^{-3} Pa s^{-1}, black contour interval is 1.5×10^{-2} Pa s^{-1} with absolute maximum at 0.2 Pa s^{-1}. Dots indicate statistical insignificance at the 5% level based on a Student's t-test.

tropics (around the equator), including a reduction over the Indo-Pacific region (75°E − 120°E, Figure 1a, brown shades) and an intensification over the Pacific ocean (160°E − 80°W, Figure 1a, green shades). During DJF, while the response in net precipitation in the deep tropics is not as strong as in JJA, a similar zonal shift is still visible with strong moistening over the Pacific Ocean (140°E − 80°W, Figure 1b), in contrast to the weaker responses over the Indian Ocean (40°E − 100°E).

To better understand these zonally dependent changes in net precipitation, $\Delta(P-E)$, we analyze the changes in the vertically integrated moisture budget, that can be written as $\overline{(P-E)} = (\rho_w g)^{-1}\left(-\nabla\cdot\int_0^{p_s}\overline{q}\overline{\mathbf{v}}dp - \nabla\cdot\int_0^{p_s}\overline{(\mathbf{v}'q')}dp\right)$, where ρ_w is the density of water, q is specific humidity, p_s is the surface pressure, overbars indicate climatological monthly means and primes indicate departure from the monthly mean (Seager et al., 2010; Trenberth & Guillemot, 1995). The change in net precipitation, $\Delta(P-E)$, can be decomposed into three components: thermodynamic (ΔTH), dynamic (ΔDYN) and transient eddies (ΔTE), where Δ denotes the difference between the (2080–2099) and (1980–1999) periods. The three components are defined as

$$\Delta TH = (\rho_w g)^{-1}\left(-\nabla\cdot\int_0^{p_s}(\mathbf{v}_{mean}\Delta q)\,dp\right), \quad (7)$$

$$\Delta DYN = (\rho_w g)^{-1}\left(-\nabla\cdot\int_0^{p_s}(\Delta\mathbf{v}q_{mean})\,dp\right), \quad (8)$$

$$\Delta TE = (\rho_w g)^{-1}\left(-\nabla\cdot\int_0^{p_s}\Delta\overline{(\mathbf{v}'q')}dp\right), \quad (9)$$

where subscript "mean" denotes the average of the (2080–2099) and (1980–1999) periods. The transient eddy component is calculated as the residual in the moisture budget equation.

The moisture budget allows one to separately analyze the effects of thermodynamic (ΔTH, changes in moisture content), dynamic (ΔDYN, changes in time mean circulation) and transient eddies (ΔTE, departures from the monthly mean) processes on the net precipitation response. The transient eddy component is found to be relatively insignificant in the deep tropics (Figure S4 in Supporting Information S1), and thus here we focus on the two other significant terms: the thermodynamic and dynamic components.

Given that the changes in net precipitation are more robust during Southern Hemisphere winter, we first focus on JJA. Figures 2a and 2b show the dynamic and thermodynamic components of the net precipitation response in JJA, respectively (colored contours). Similar to previous studies (Seager et al., 2010), both thermodynamic and dynamic components contribute to the total precipitation response (Figure 1a), with the dynamic component dominating over the tropical Pacific and Indian Oceans. In particular, the thermodynamic component (Figure 2b), driven by the change in specific humidity, contributes to the precipitation increase in the ITCZ and drying of the subtropics (Held & Soden, 2006; Seager et al., 2010). Additionally, changes in the moisture gradient cause drying in the margins of convection zones (Neelin et al., 2003). Conversely, the dynamic component (Figure 2a), controlled by changes in the circulation, explains the zonal asymmetry in the response in the deep tropics (Figure 1a), that is, the equatorial drying in the Indo-Pacific and Indian Ocean regions and the moistening of the Central and East Pacific. The dynamic component can be decomposed to show the contributions from the meridional and zonal components of the circulation separately, by using the divergent component of their velocities, u_{div}, v_{div}, derived using a Helmholtz decomposition (Figures 2c and 2d). It is clear that the meridional component of the circulation is of much larger significance, highlighting its high impact on the dynamical component of the projected changes in net precipitation. Note that the rotational component contribution to changes in the dynamic component of the net precipitation is negligible compared to the contribution of the divergent component (see Figure S5 in Supporting Information S1).

The dependence of the zonal shift in the deep tropical net precipitation on dynamic processes, and specifically on the meridional component, motivates the further examination of the large-scale tropical circulation. The effect of the large-scale flow on the precipitation response to anthropogenic emissions might stem from changes in both the meridional and zonal circulations. We thus follow previous studies (Keyser et al., 1989; Schwendike et al., 2014), and decompose the 500 hPa vertical velocity into two components: the vertical velocity associated with the meridional circulation (ω_θ), and the vertical velocity associated with the zonal circulation (ω_ϕ) (Figures 2e and

2f). This method allows us to quantify the contribution of each dynamic component to the changes in precipitation. The response of the decomposed vertical velocity is defined here similarly to the precipitation response, that is, the differences between the last 20 years in the 21st and 20th centuries, and is shown in the colored contours in Figures 2e and 2f. Black lines represent the historical values, where solid lines denote descent (positive values), and dashed lines denote ascent (negative values). An overlap between colored contours and black lines of the same sign indicates strengthening of the ascent (descent), and opposing signs indicate weakening of the ascent (descent). In the center of the equatorial Pacific, we note the resemblance between the region of increased precipitation (green area in Figure 2a) and the region where there is net strengthening of the ascent (blue area Figure 2e), including areas with increased ascending motion (blue over dashed) and with reduced descending motion (blue over solid), is associated with increased net precipitation (Figure 1a). A weakening of the ascent is visible in the Indo-Pacific region (Figure 2e), which results in a decrease in net precipitation (Figure 1a). Therefore, the meridional component is the main component of the tropical precipitation changes, where a shift in the ascending region of the meridional circulation is linked to a shift in the net precipitation. The zonal component, on the other hand, has a minor effect on the vertical velocity changes in these tropical regions (Figure 2f).

Not only do changes in the ascending branch of the meridional circulation affect the longitudinally dependent precipitation response, but changes in the descending branch as well. For example, as noted in previous studies (e.g., Staten et al., 2019), the expansion of the meridional circulation (Figure 2a, difference between the 20th century values in gray dashed lines and 21st century values in gray solid lines) exhibits strong longitudinal dependence, with the most significant expansion occurring in the center of the equatorial Pacific, where most of the increase in net precipitation occurs (the edge of the circulation is defined where the longitudinally dependent meridional circulation is 20% of its global maximum absolute values at 500 hPa, considering only the stronger winter cell). In this region, the circulation during the 20th century is very narrow and almost non-existent (170° W–140°W, Figure S6a in Supporting Information S1, gray dotted line). Therefore, a region that was outside of the HC in the 20th century will reside inside the HC by the end of the 21st century, due to the descending branch of the meridional circulation expanding southward. This expansion enlarges the area of the circulation, where the descending and ascending branches are now farther apart, and is associated with the increase in net precipitation over the center of the Pacific.

Future changes in net precipitation are also found to be associated with shifts in the meridional circulation during DJF. Similarly to JJA, during DJF, when comparing the thermodynamic and dynamic components of the net precipitation response (Figures S6a and S6b in Supporting Information S1), the dynamic component dominates the zonal asymmetries in the tropics. In addition, the decomposition of the dynamic component to zonal and meridional contribution shows great similarity to JJA, where the meridional component is much more significant than the zonal component (Figures S6c and S6d in Supporting Information S1). The decomposition of the vertical velocity in DJF yields similar results to JJA, where the response of the meridional component (Figure S6e in Supporting Information S1) exhibits a pattern that is similar to the dynamic precipitation response (Figure S6a in Supporting Information S1), with the zonal component being less significant than the meridional one (Figure S6f in Supporting Information S1). The two seasons differ in the expansion of the meridional circulation. During DJF, the edge of the circulation is not visible in the east and center of the Pacific (Figure S6a in Supporting Information S1), due to the circulation being significantly weaker in that area. Moreover, the expansion of the HC in DJF is less significant than in JJA. As a result, in comparison to JJA, the dynamic component in DJF yields a weaker strengthening in the central Pacific. Nonetheless, the linkage between the longitudinal variations in the meridional circulation, as indicated by the vertical velocity, and the response of the precipitation is prominent in both seasons.

3.2. Lagrangian Analysis of the Three-Dimensional Tropical Large-Scale Circulation

In order to demonstrate that the shift of the meridional circulation, which is detected in the vertical velocity (Figure 2e), is dominant in setting the changes in the three dimensional tropical circulation, we take also a Lagrangian approach in which the air parcel trajectories are calculated for relevant initial locations. In particular, we calculate the location of each air parcel every 6 hr, using the time averaged velocity field over the 1980–1999 and 2080–2099 periods, which yields the air parcels' path. The response of the three-dimensional circulation to anthropogenic emissions is revealed in the difference between the 20th century trajectories (Figures 3a–3c) and the 21st century trajectories (Figures 3d–3f). Based on the zonal shift in the ascending region of the meridional

circulation (Figure 2e), we choose three representative regions for initial air parcel positions (Figure 3, black dots). All air parcels are initiated at the 500 hPa pressure level. The first region is at the equatorial Indo-Pacific (70°E−110°E, Figures 3a and 3d), where the 20th century meridional circulation is most intense, and the vertical velocity is projected to weaken by 2100 (Figures 2a and 2e). The second region is in the mid-west Pacific (160°E−160°W, Figures 3b and 3e), where the circulation and net precipitation are projected to strengthen (Figures 2a and 2e). The third region is in the mid-east Pacific (150°W–110°W, Figures 3c and 3f), where the 20th century meridional circulation is insignificant, as visible from the edge of the meridional circulation (Figure 3, gray dotted line). By the end of the 21st century, the expansion of the meridional circulation places this region within the circulation, with air parcels participating in the tropical conveyor belt, thus, together with the zonal shift of the meridional flow, are associated with strengthening the net precipitation over that region (Figure 2e).

The future weakening of the circulation is apparent in the first region (compare Figures 3a and 3d) where the main movement in the tropical conveyor belt is initialized. The 21st century trajectories not only extend less south and east compared to the 20th century trajectories, but also the net precipitation decreases (Figure 2a), revealing the connection between the weakening of the three-dimensional circulation and the net precipitation response. In the second region (Figures 3b and 3e), where the net precipitation increases (Figure 2a), the 21st century air parcels ascend to higher altitudes, move farther to the south and then much farther to the east, thus indicating a strengthening of the circulation associated with an increase in net precipitation (Figure 2c). In the third region (Figures 3c and 3f), the 20th century air parcels that are outside of the ascending region of the HC and descend to lower altitudes, while the 21st century air parcels that are now inside the HC, move westward, ascend, and later on move poleward, therefore participating in the tropical conveyor belt. This analysis shows that the shift in the vertical velocity, related to the meridional circulation, appears in the three-dimensional circulation, as can be seen from the difference between the top and bottom rows of Figure 3. This shift is shown to involve large-scale changes in the meridional air movement that goes well outside the deep tropical region. While further investigation is needed to determine what causes these changes in the meridional circulation, our analysis confirms that zonal shifts in the meridional circulation (and not the zonal circulation) are the main contributors to the tropical net precipitation response to anthropogenic emissions.

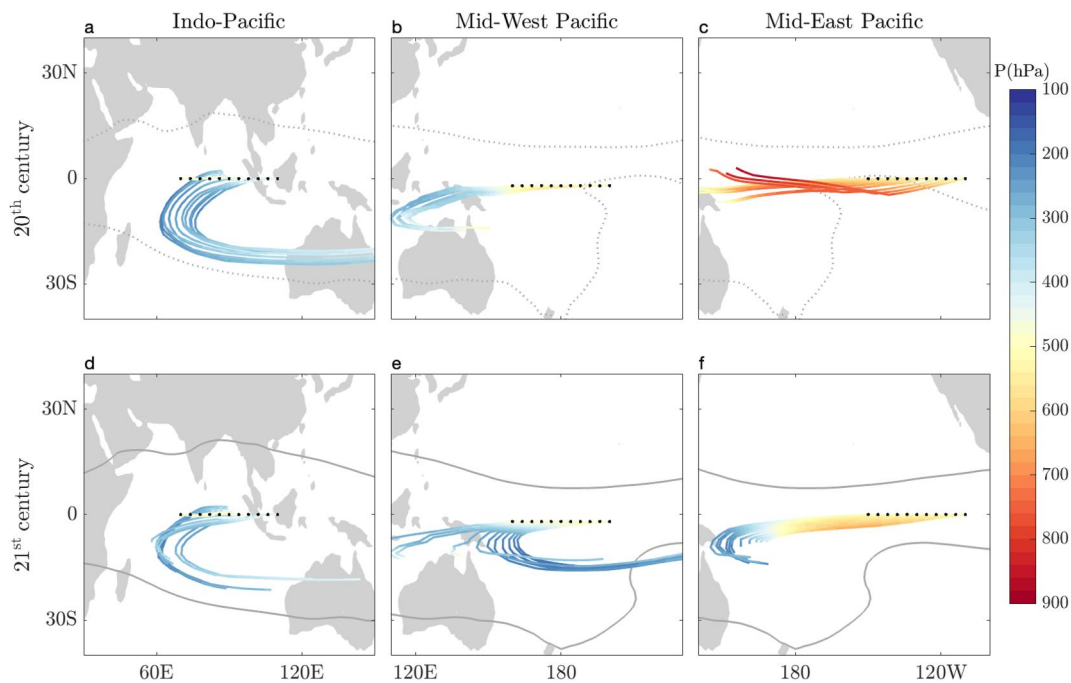

Figure 3. Trajectories calculated for the 1980–1999 period (a–c) and the 2080–2099 period (d–f) in JJA. Black dots mark the starting position of the air parcel, and colors indicate height in pressure coordinate. Each air parcel is initialized at 500 hPa and tracked for 20 days. Gray dashed and solid contours indicate the edge of the meridional circulation over the 1980–1999 and 2080–2099 periods, respectively.

4. Discussion

We show that the zonal shift in the net tropical precipitation, in response to anthropogenic emissions, is mainly associated with the projected changes in the ascending and descending branches of the meridional circulation. This dynamical behavior is revealed only when decomposing the large-scale tropical circulation to its zonal and meridional components. One sensitivity of our study can arise from the fact that we use the two-dimensional decomposition method (e.g., Schwendike et al., 2014), while some of the previous studies used a three-dimensional method (e.g., Hu et al., 2017). Comparing the three-dimensional method to the two-dimensional, Hu et al. (2017) found that quantitatively there are some differences between the circulations, especially for the zonal circulation, but qualitatively similar patterns arise, and these quantitative differences do not affect our conclusions.

Given these large climate impacts of the meridional circulation, analyzing the entire three-dimensional circulation can have important consequences for other aspects of the tropical climate system, such as El-Niño, Monsoons, and the Madden-Julian Oscillations. Moreover, since the changes in the longitudinally dependent meridional circulation, as seen in the 3D Lagrangian analysis, extended well beyond the deep tropical region, they will also affect the extratropics. The explanation given here for the projected changes in tropical precipitation stresses the importance of both treating the tropical circulation as a 3D flow (and not as the zonally symmetric Hadley circulation), and of better monitoring the longitudinal variations in the meridional circulation under climate change.

Data Availability Statement

CMIP6 data used in this manuscript is available at Eyring et al. (2016). The code used in this manuscript is available via GitHub: https://github.com/danaraiter/Code_for_manuscript_Raiter_etal_2022.

Acknowledgments
We acknowledge support from the Israeli Science Foundation (Grant 996/20).

References

Byrne, M. P., & O'Gorman, P. A. (2015). The response of precipitation minus evapotranspiration to climate warming: Why the "wet-get-wetter, dry-get-drier" scaling does not hold over land. *Journal of Climate*, *28*(20), 8078–8092. https://doi.org/10.1175/JCLI-D-15-0369.1

Chadwick, R., Boutle, I., & Martin, G. (2013). Spatial patterns of precipitation change in CMIP5: Why the rich do not get richer in the tropics. *Journal of Climate*, *26*(11), 3803–3822. https://doi.org/10.1175/jcli-d-12-00543.1

Chemke, R., & Polvani, L. M. (2019). Opposite tropical circulation trends in climate models and in reanalyses. *Nature Geoscience*, *12*(7), 528–532. https://doi.org/10.1038/s41561-019-0383-x

Chou, C., & Neelin, J. D. (2004). Mechanisms of global warming impacts on regional tropical precipitation. *Journal of Climate*, *17*(13), 2688–2701. https://doi.org/10.1175/1520-0442(2004)017⟨2688:MOGWIO⟩2.0.CO;2

Chou, C., Neelin, J. D., Chen, C.-A., & Tu, J.-Y. (2009). Evaluating the "rich-get-richer" mechanism in tropical precipitation change under global warming. *Journal of Climate*, *22*(8), 1982–2005. https://doi.org/10.1175/2008jcli2471.1

Collins, M., Knutti, R., Arblaster, J., Dufresne, J.-L., Fichefet, T., Friedlingstein, P., et al. (2013). Long-term climate change: Projections, commitments and irreversibility [Book Section]. In T. Stocker, D. Qin, M. Tignor, S. K. Allen, Y. Xia, V. Bex, et-al. (Eds.), *Climate change 2013: The physical science basis. contribution of working group i to the fifth assessment report of the intergovernmental panel on climate change* (pp. 1029–1136). Cambridge University Press.

Eyring, V., Bony, S., Meehl, G. A., Senior, C. A., Stevens, B., Stouffer, R. J., & Taylor, K. E. (2016). Overview of the coupled model intercomparison project phase 6 (CMIP6) experimental design and organization [Dataset]. Geoscientific Model Development, *9*, 1937–1958. https://doi.org/10.5194/gmd-9-1937-2016

Fuselier, E. J., & Wright, G. B. (2009). Stability and error estimates for vector field interpolation and decomposition on the sphere with rbfs. *SIAM Journal on Numerical Analysis*, *47*(5), 3213–3239. https://doi.org/10.1137/080730901

Galanti, E., Raiter, D., Kaspi, Y., & Tziperman, E. (2022). Spatial patterns of the tropical meridional circulation: Drivers and teleconnections. *J. Geophys. Res. (Atmos.)*, *127*(2), e2021JD035531. https://doi.org/10.1029/2021JD035531

Hartmann, D. L. (2016). Chapter 6–Atmospheric general circulation and climate. In *Global physical climatology* (2nd ed., pp. 159–193). Elsevier.

Held, I. M., & Soden, B. J. (2006). Robust responses of the hydrological cycle to global warming. *Journal of Climate*, *19*(21), 5686–5699. https://doi.org/10.1175/jcli3990.1

Hu, S., Cheng, J., & Chou, J. (2017). Novel three-pattern decomposition of global atmospheric circulation: Generalization of traditional two-dimensional decomposition. *Climate Dynamics*, *49*(9–10), 3573–3586. https://doi.org/10.1007/s00382-017-3530-3

Karnauskas, K. B., & Ummenhofer, C. C. (2014). On the dynamics of the Hadley circulation and subtropical drying. *Climate Dynamics*, *42*(9), 2259–2269. https://doi.org/10.1007/s00382-014-2129-1

Keyser, D., Schmidt, B. D., & Duffy, D. G. (1989). A technique for representing three-dimensional vertical circulations in baroclinic disturbances. *Monthly Weather Review*, *117*(11), 2463–2494. https://doi.org/10.1175/1520-0493(1989)117<2463:atfrtd>2.0.co;2

Lu, J., Vecchi, G. A., & Reichler, T. (2007). Expansion of the Hadley cell under global warming. *Geophysical Research Letters*, *34*(6). https://doi.org/10.1029/2006gl028443

Lucas, H., & Nguyen, H. C. (2015). Regional characteristics of tropical expansion and the role of climate variability. *Journal of Geophysical Research: Atmosphere*, *120*(14), 6809–6824. https://doi.org/10.1002/2015jd023130

Mamalakis, A., Randerson, J. T., Yu, J.-Y., Pritchard, M. S., Magnusdottir, G., Smyth, P., et al. (2021). Zonally contrasting shifts of the tropical rain belt in response to climate change. *Nature Climate Change*, *11*(2), 143–151. https://doi.org/10.1038/s41558-020-00963-x

Neelin, J. D., Chou, C., & Su, H. (2003). Tropical drought regions in global warming and El Niño teleconnections. *Geophysical Research Letters*, *30*(24). https://doi.org/10.1029/2003gl018625

Nguyen, H., Hendon, H. H., Lim, E. P., Boschat, G., Maloney, E., & Timbal, B. (2018). Variability of the extent of the Hadley circulation in the southern hemisphere: A regional perspective. *Climate Dynamics*, *50*(1), 129–142. https://doi.org/10.1007/s00382-017-3592-2

Raiter, D., Galanti, E., & Kaspi, Y. (2020). The tropical atmospheric conveyor belt: A coupled eulerian-lagrangian analysis of the large-scale tropical circulation. *Geophysical Research Letters*, *47*(10), e2019GL086437. https://doi.org/10.1029/2019gl086437

Schwendike, J., Govekar, P., Reeder, M. J., Wardle, R., Berry, G. J., & Jakob, C. (2014). Local partitioning of the overturning circulation in the tropics and the connection to the Hadley and Walker circulations. *Journal of Geophysical Research: Atmosphere*, *119*(3), 1322–1339. https://doi.org/10.1002/2013jd020742

Seager, R., Naik, N., & Vecchi, G. A. (2010). Thermodynamic and dynamic mechanisms for large-scale changes in the hydrological cycle in response to global warming. *Journal of Climate*, *23*(17), 4651–4668. https://doi.org/10.1175/2010jcli3655.1

Staten, P. W., Grise, K. M., Davis, S. M., Karnauskas, K., & Davis, N. (2019). Regional widening of tropical overturning: Forced change, natural variability, and recent trends. *Journal of Geophysical Research: Atmosphere*, *124*(12), 6104–6119. https://doi.org/10.1029/2018jd030100

Trenberth, K. E., & Guillemot, C. J. (1995). Evaluation of the global atmospheric moisture budget as seen from analyses. *Journal of Climate*, *8*(9), 2255–2272. https://doi.org/10.1175/1520-0442(1995)008<2255:eotgam>2.0.co;2

Vallis, G. K., Zurita-Gotor, P., Cairns, C., & Kidston, J. (2015). Response of the large-scale structure of the atmosphere to global warming. *Quarterly Journal of the Royal Meteorological Society*, *141*(690), 1479–1501. https://doi.org/10.1002/qj.2456

Vecchi, G. A., & Soden, B. J. (2007). Global warming and the weakening of the tropical circulation. *Journal of Climate*, *20*(17), 4316–4340. https://doi.org/10.1175/jcli4258.1

Waugh, D. W., Grise, K. M., Seviour, W. J. M., Davis, S. M., Davis, N., Adam, O., et al. (2018). Revisiting the relationship among metrics of tropical expansion. *Journal of Climate*, *31*(18), 7565–7581. https://doi.org/10.1175/jcli-d-18-0108.1

Zhang, G., & Wang, Z. (2013). Interannual variability of the Atlantic Hadley circulation in boreal summer and its impacts on tropical cyclone activity. *Journal of Climate*, *26*(21), 8529–8544. https://doi.org/10.1175/jcli-d-12-00802.1